https://doi.org/10.1142/9789811278952_0003

Chapter 3

Upgrade of the Experimental Detectors for High Luminosity LHC

F. Hartmann[a], B. Hippolyte[b], F. Lanni[c], T. Nayak[d], C. Parkes[e] and P. Rumerio[f]

[a]*Karlsruhe Institute of Technology, 76131 Karlsruhe, Germany*
[b]*USIAS - Université de Strasbourg, 67081, France and CERN, Switzerland*
[c]*Brookhaven National Laboratory, Upton, NY 11973, USA*
[d]*National Institute of Science Education and Research, Bhubaneswar, Odisha 752050, India and CERN, Switzerland*
[e]*University of Manchester, Manchester M13 9PL, UK*
[f]*University of Alabama, AL 35487, USA and Università di Torino, 10124, Italy*

The HL-LHC upgrade plans of ALICE, ATLAS, CMS and LHCb are briefly outlined in this chapter.

1. Introduction

The high-luminosity upgrade of the LHC (HL-LHC)[1–3] will enable the four experiments to enter a new era, allowing searches of new phenomena and precision measurements.

ATLAS and CMS will upgrade their detector systems to cope with a pileup of 200 collisions per bunch crossing, corresponding to an ultimate, leveled instantaneous luminosity of $\mathcal{L} = 7.5 \times 10^{34}$ cm^{-2}s^{-1}, and to an integrated luminosity of 4 ab^{-1}. These conditions will pose unprecedented challenges in terms of particle rates and radiation levels: L1 trigger rates will reach up to approximately 1 MHz, while the inner tracking detectors will be designed to withstand fluence up to 2.3×10^{16} n$_{\mathrm{eq}}$/cm^2 and total ionizing doses in excess of 1 Grad. Plans will be described in Sections 2 and 3 respectively.

Section 4 describes the proposed LHCb Upgrade II detector, which would operate at an instantaneous luminosity of 1.5×10^{34} cm^{-2} sec^{-1}, almost an order of magnitude above Upgrade I, for a minimum of 300 fb^{-1} integrated luminosity.

Finally, ALICE is completing major upgrades for long shutdown 2 (LS2) that will result in a more precise, reliable, and faster experimental setup in the HL-LHC era, as summarized in Section 5. High statistics Pb–Pb data, amounting to at least 13 nb^{-1}, will be accumulated, together with O-O, pp, p-O and p-Pb collisions. The future plan after Run-4 calls for a compact, next-generation multipurpose detector as a follow-up to the ALICE experiment, conceived to handle luminosities a factor of 20 to 50 times higher than RUN-3.

2. The HL-LHC Upgrade of the ATLAS Detector

The ATLAS Phase-II upgrades, illustrated concisely in Figure 1, are designed to cope with the conditions expected for the ultimate HL-LHC configuration with up to $\mu = 200$ inelastic collisions per bunch crossing.

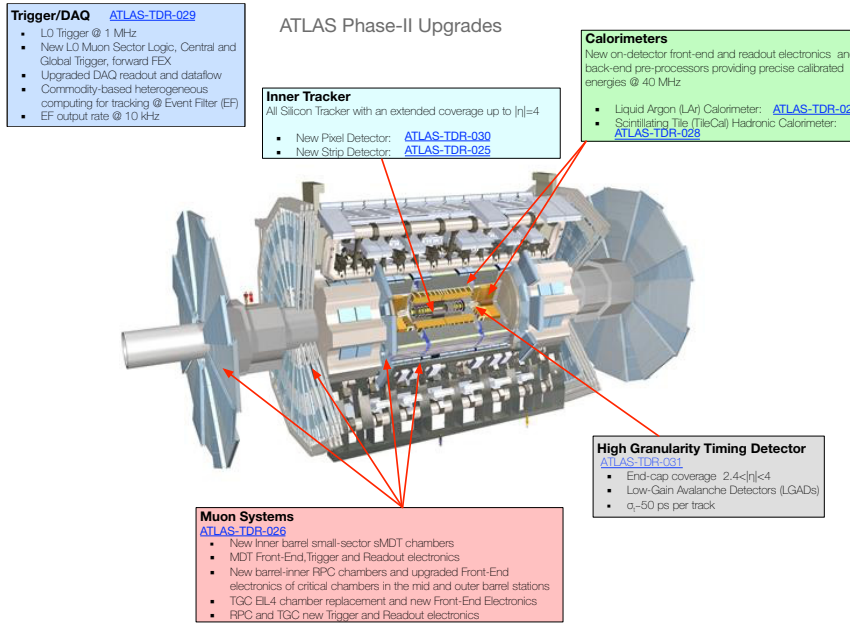

Fig. 1. ATLAS detector and the HL-LHC upgrade programme of its sub-systems.

2.1. *Inner Tracker*

The Inner Tracker (ITk) layout is shown in Figure 2. Five layers of pixel detector modules are installed at the inner radii around the beam pipe in the barrel region. Several pixel rings in the forward region extend the pseudo-rapidity coverage of the tracker system to $|\eta| < 4$. The outer tracker is made of four barrel layers and six end-cap disks of strip detectors modules on both sides of the layers, covering a pseudo-rapidity range of $|\eta| < 2.7$. The Pixel and Strip Detector volumes are separated by a Pixel Support Tube (PST). The ITk layout has been optimised to reach, at the HL-LHC conditions, similar or better performance as the present tracker: to cope with the higher pileup, the granularity of the sensors is increased, resulting in an average occupancy of 0.16% in the Pixel and 1.2% in the Strip detectors. The ITk design targets to have about half as much material compared to the current ID, minimising the effects of losses due to hadronic interactions and bremsstrahlung.

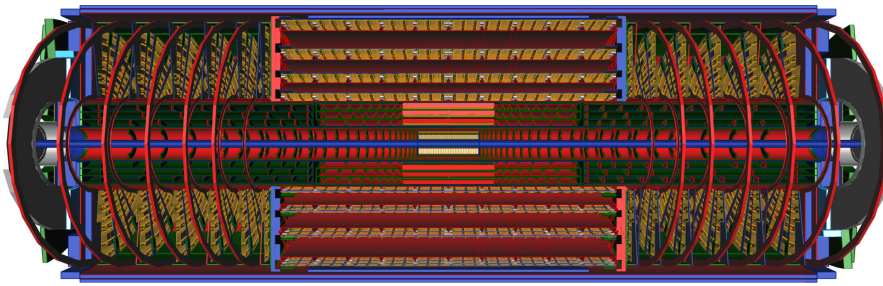

Fig. 2. Layout of the HL-LHC Inner Tracker (ITk) of ATLAS.

2.1.1. *ITk Pixel Detector*

The design of the ITk-Pixel system[4] features a short central barrel region, inclined modules that cover the intermediate η-region, and rings perpendicular to the beam direction in the very forward region.

The innermost two Pixel layers are designed to be replaceable, as the maximum expected neutron fluence exceeds 2×10^{16} 1MeV $n_{eq}cm^{-2}$. Different sensor technologies are used in the different regions of the detector: 3D sensors and thin (100 μm) n-in-p planar sensors in the inner layers, 150 μm thick n-in-p planar sensors in the outer three layers and in the end-cap rings. The pixel size

is $25 \times 100\,\mu m^2$ in the central barrel region of the first layer and $50 \times 50\,\mu m^2$ elsewhere.

Pixel modules are made by bump-bonding the silicon sensors on the front-end read-out ASICs, fabricated in 65 nm CMOS technology. The modules are glued to a flex circuit interfacing to the readout data transmission, and power distribution systems.

2.1.2. *ITk Strip Detector*

The ITk outer system is made of approximately 18000 modules of silicon Strip sensors.[5] A module is built by gluing kapton flexible hybrids to the sensors. The hybrids also host the readout ASICs in 130 nm CMOS technology. The modules are assembled onto CO_2 cooled carbon fibre structures ("staves" and "petals", respectively, in the barrel and end-cap regions).

392 staves are installed in the four barrel layers. Each barrel stave is populated with 28 Strip modules on both the top and bottom side. The Strip sensors are 24.1 mm long (short-strips) in the two innermost layers, and 48.2 mm (long-strips) in the outer two.

In the end-caps 32 identical petals, each housing 9 modules on each side, are assembled on every disk. Six different sensor geometries allow to cover the wedge-shaped petal surface, i.e. pointing to the beam axis.

2.2. *Calorimeters*

The on-detector and off-detector readout electronics of both the Liquid Argon (LAr) and Tile (TileCal) calorimeters[6,7] are entirely replaced during the Phase-II upgrades (Figure 3). In the new readout scheme, after a first stage of (pre)-amplification, the signals are split into two overlapping linear gain scales, filtered by shaping amplifiers and digitized at 40 MHz. The digitized samples are multiplexed and transmitted off-detector optically to pre-processor modules, where energy and time of the deposits in the calorimeter elements are reconstructed at each bunch crossing.

In the LAr system 1524 new Front-End Boards (FEB2s) are installed on detector, each processing the signals from 128 calorimeter cells. 372 LAr Signal Processor (LASP) modules receive off-detector the front-end data through approximately 31900 fibers, for a throughput in excess of 280 Tb/s. In addition,

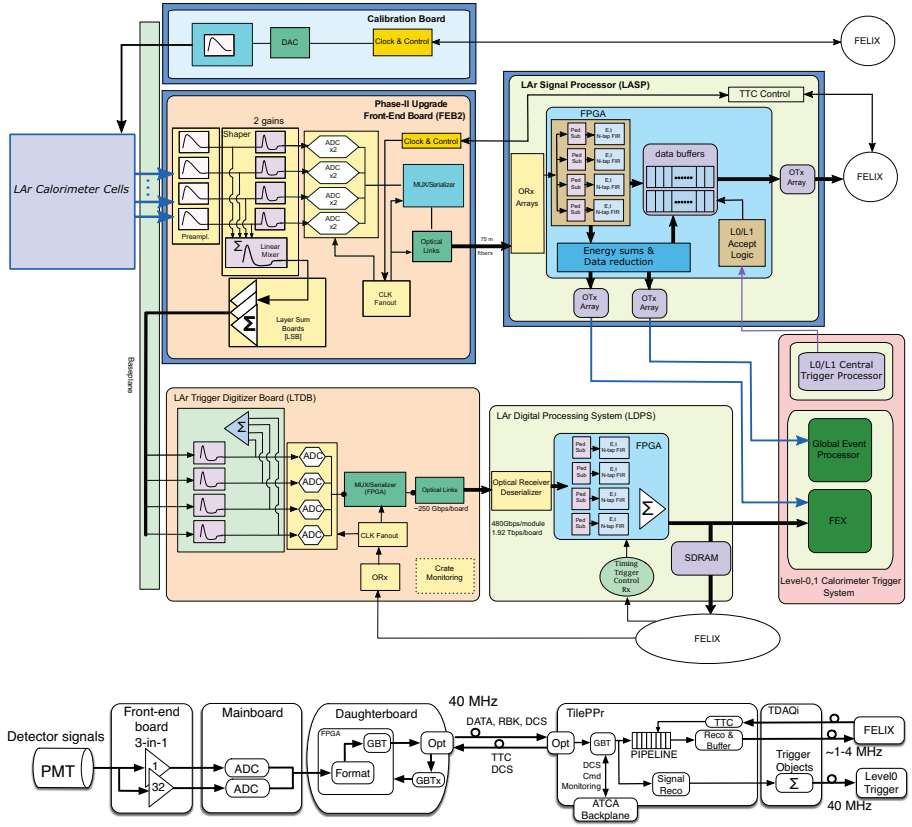

Fig. 3. High-level diagrams of the LAr (top) and TileCal (bottom) calorimeter readout.

an upgraded calibration system allows to inject calibration signals directly into the LAr cells with a precision better than 0.1% over the full 16-bit dynamic range.

In TileCal the PMTs, the front-end electronics, the power, and the cooling services are supported by new mechanical structures, segmented in four independent "Mini-drawers", each servicing a TileCal module, i.e. one of the 256 wedges constituting the barrel and end-cap detectors. A total of 4096 fibres, each running at 9.6 Gb/s bandwidth – i.e. for a total of 1.3 Tb/s throughput, interface the on-detector front-end to 32 PPr modules. The off-detector PPr modules interface to the DAQ system and to the Level-0 Trigger processors through the TDAQi modules.

2.3. *Muon Detectors*

The main challenge for the ATLAS Muon Spectrometer[8] is to maintain excellent selection and tracking capability at the HL-LHC conditions in terms of background rates, pile-up and integrated radiation doses. Figure 4 shows the spectrometer upgraded detectors in the two orthogonal planes.

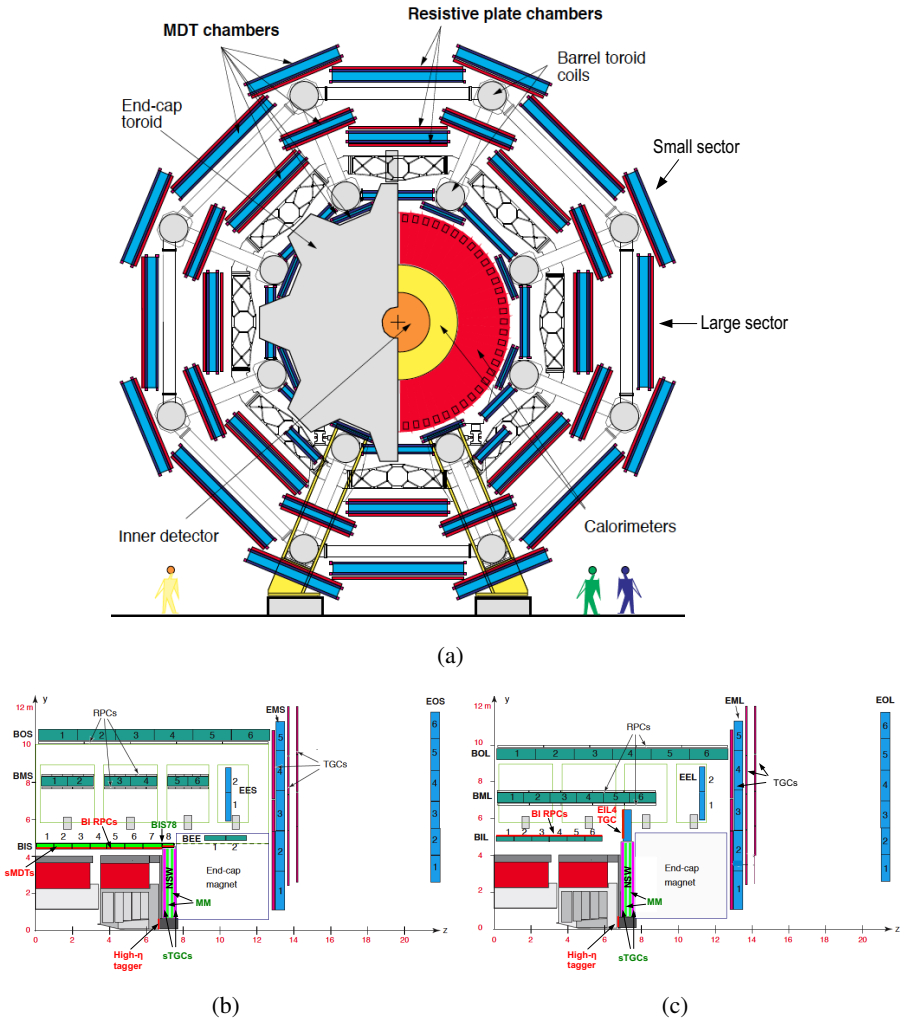

Fig. 4. Muon spectrometer layout in the r-ϕ plane (a), and in the r-z plane for the small (b) and large (c) sectors respectively.

2.3.1. *RPC and MDT upgrades in the barrel spectrometer*

New Resistive Plate Chambers (RPC) with increased rate capability are installed in the inner barrel layer (BI) to improve the acceptance and robustness of the trigger selection. The installation of the BI chambers is challenging in terms of available space, in particular in the small sectors of the muon spectrometer, where it is possible only if the existing Monitored Drift Tubes (MDT) chambers are replaced with new small diameter MDT (sMDT) detectors. Also, selected RPC chambers in the middle (BM) and outer barrel (BO) layers in the areas of highest rate, i.e. at $|\eta| > 0.8$, are refurbished during the winter shutdowns after LS3, with new electronics and readout planes, to operate the chambers at reduced high voltage without efficiency loss.

2.3.2. *TGC upgrade in the barrel-endcap transition*

In the barrel-endcap transition region new Thin Gap Chambers (TGC) triplets replace the current TGC doublets (EIL4 in Figure 4c). The triplets, with finer readout granularity, allow to implement a more robust majority logic, i.e. requiring hits in two out of three planes, and to use a smaller coincidence window, suppressing the rate of random coincidences generated by low-p_T charged particles (typically slow protons) produced inside the endcap toroid cryostats.

2.3.3. *Electronics upgrades*

A large fraction of the on- and off-detector readout and trigger electronics is upgraded for compatibility with the Level-0 trigger requirements. The RPC and TGC trigger and readout chains are redesigned with data streamed off-detector and made available to the Level-0 trigger processors. The front-end electronics of the MDT detectors is also upgraded: raw data are sent to dedicated processors where precise measurements of the hit coordinates allow the Level-0 trigger processor to sharpen trigger efficiency turn-on curves at high p_T, and reduce the background rate significantly.

2.4. *High Granularity Timing Detector*

The High Granularity Timing Detector (HGTD) is a precision timing system based on Low Gain Avalanche Detectors (LGAD), installed in the region $2.4 <$

$|\eta| < 4.0$.[9] It improves the rejection of pileup jets with $30 < p_{\mathrm{T}} < 50$GeV in the forward region up to a factor of 40% at the start of the detector lifetime to 25% at the end of lifetime, and reduces the inefficiencies of forward lepton isolated tracks by a factor two. HGTD comprises two layers of pixelated sensors (1.3×1.3 mm^2) installed on the end-cap cryostats for an active area of 6.3 m^2 (see Figure 5a). Full-sized (15×15) LGAD arrays, shown in Figure 5c, have achieved in testbeams a time resolution of 30 ps.

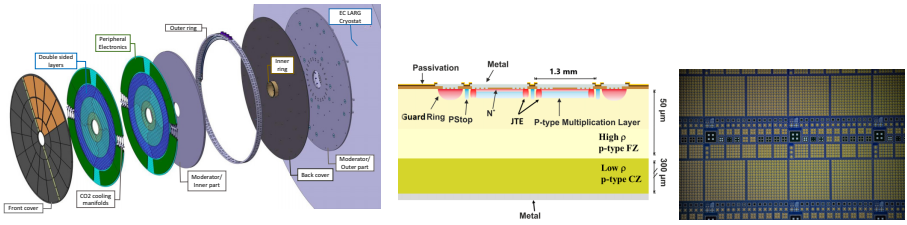

(a) (b) (c)

Fig. 5. (a) HGTD detector layout and mechanical structure. (b) Cross-section of an LGAD sensor including a JTE around each sub-pad. (c) Microscope picture of an HGTD LGAD prototype with full size sensors (15×15 array) tested on beam.

2.5. *Trigger and DAQ*

The baseline configuration[10] features a Level-0 (L0) hardware trigger with a readout rate of 1 MHz and a latency of 10 µs, followed by the Event Filter (EF) system performing the final event selection, and outputting data at 10 kHz - see Figure 6.

2.5.1. *Level-0 Trigger System*

The existing Muon Trigger processors are entirely replaced with upgraded modules that process the information from the RPC, TGC and sTGC and MicroMegas detectors in the forward region (New Small Wheel). They are complemented by additional processors that improve the precision of the muon p_T measurement using the information of the MDT detectors.

The Phase-I Calorimeter Feature Extractors (FEXes) modules are maintained during the HL-LHC operations, and their firmware optimized for the

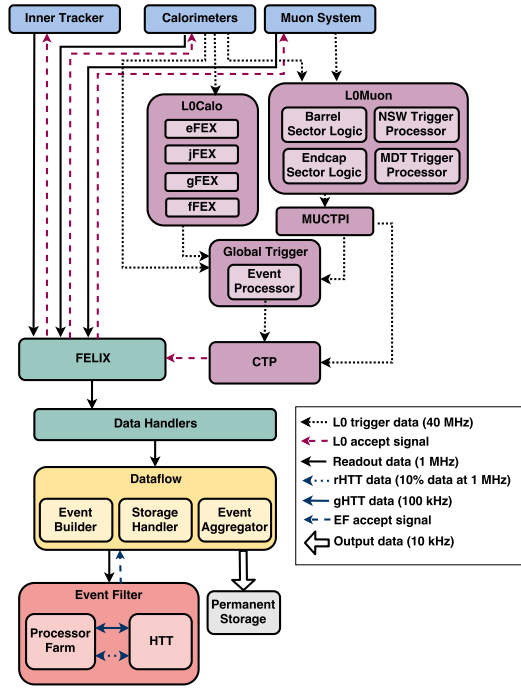

Fig. 6. High-level diagram of the Trigger/DAQ architecture.

expected pile-up conditions and the extra-latency available in Run-4. Additional FEXes units are installed to process data from the forward calorimeter.

The Global Trigger system performs offline-like algorithms, and executes topological algorithms extending the functionality of the Run-2 Topological Processor.

2.5.2. *Data Acquisition System*

Detector data are transmitted to the Front-End Link eXchange (FELIX) nodes, a common interface between the detector-specific links and the commodity network downstream. Along the network, data are received by the Data Handlers, where detector-specific processing is implemented, and transferred to the Dataflow sub-system, which transports, aggregates, buffers and compresses event data for utilization in the EF. The system is designed to sustain a throughput of 5.2 TB/s.

2.5.3. *Event Filter System*

The Event Filter (EF) system, a large commodity CPU-based processing farm, is upgraded to maintain the rejection by employing offline-type particle reconstruction, and achieve an output rate of 10 kHz. The total data throughput to storage is 60 GB/s.

The design of the EF tracking sub-system described in the TDAQ Technical Design Report (TDR) was based on a custom-electronics Hardware Tracking for the Trigger (HTT) based on Associative Memory ASICs deployed on ATCA processing modules.[10] Recently, the baseline design has changed in favor of a commodity solution that may benefit of accelerators as co-processors. The opportunity to drop tight latency constraints, originally required by the optional use of tracking in earliest stage of the trigger chain, has been the driving reason behind the decision of this baseline change. A TDR amendment is in preparation and its release is planned at the beginning of 2022.

3. The HL-LHC Upgrade of the CMS Detector

To exploit the high-luminosity upgrade of the LHC, the CMS experiment has to combat higher overall particle rates, higher pileup of superimposed proton-proton collision events per LHC bunch crossing, and higher instantaneous and integrated radiation doses to the detector elements. All CMS systems for the HL-LHC (CMS Phase-2 upgrade) are designed to withstand an integrated luminosity of 4 ab^{-1}, equivalent to a fluence of 2.3×10^{16} n_{eq} /cm^2 at the innermost radius of the Pixel detector, to cope with a pileup of 200 collisions per bunch crossing, and to sustain a Level-1 (L1) trigger rate of 750 kHz with a latency of 12.5 μs. The whole system including the trigger concept implements the Particle Flow (PF) paradigm.[11] The tracking system and endcap calorimeters will be completely replaced with much finer granularity systems and — for the first time for an all-silicon tracker detector — L1-trigger capability. The Tracker coverage will be extended to $|\eta| = 4.0$. Figure 7 gives a concise overview. A new MIP (Minimum Ionizing Particle) timing detector (MTD) will add a fourth dimension to reconstructed tracks. The barrel Electromagnetic Calorimeter will be refurbished with new electronics, which will stream data at full 40 MHz. The full Muon front-end and back-end system will be renewed to cope with the higher particle rates while the forward region will be significantly extended to $|\eta| = 2.8$.

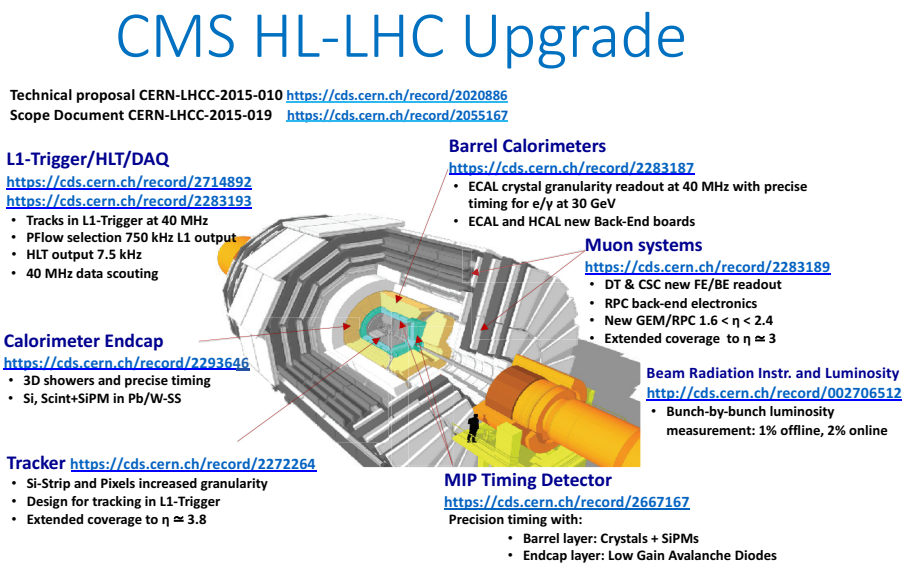

Fig. 7. The HL-LHC upgrade of the CMS detector.

3.1. *CMS Phase-2 Tracker*

The Phase-2 Tracker will consist of an Inner Pixel Tracker (IT) based on silicon pixel modules and an Outer Tracker (OT) composed of silicon modules with strip and macro-pixel sensors. The main challenge is to increase radiation tolerance, reduce mass, and increase granularity to cope with high pileup and ensure efficient tracking, two-track separation in high energetic jets, and good 3D pattern recognition. A multi-year campaign to study radiation tolerance led to the choice of *n-in-p* sensors in all OT and IT layers with the potential exception of 3D sensors for the innermost pixel layer. Many novel design choices achieve a significant reduction in material budget and, consequently, multiple scattering. This significantly improves transverse momentum (p_{T}) resolution, and lowers the photon conversion rate and electron bremsstrahlung. The main strategies to reduce mass are: implementing fewer layers, using DC-DC converters in the OT and serial power in the IT (with significant reduction of power cable mass), adopting ultra-light structural materials and CO_2 cooling (smaller pipes, lighter liquid), and reducing the number of connectors, extra boards, cables, etc. Figure 8 shows one quadrant with 4 inner pixel barrel layers plus twelve forward disks, spanning the full detector length, extending

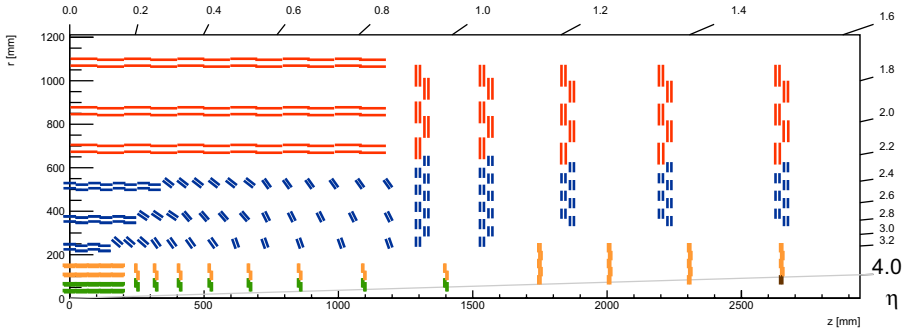

Fig. 8. The HL-LHC upgrade of the CMS Tracker. The red/blue outer layers are composed of 2S and PS p_T-modules, respectively (see Figure 9). The orange pixel layers/disks consist of 1×2 chips modules while the green ones consist of 2×2 chip modules. The Tracker, all in all, has seven pixel layers, of which 4 are based on micro- and 3 are macro-pixels. The innermost ring of endcap 12 (brown) is located beyond $|\eta| = 4.0$ and serves as an independent luminometer.[12]

the coverage to $|\eta| = 4.0$. A partially inclined geometry is implemented in the OT, saving about 5 m^2 of active elements. With respect to the existing detector, the pitch in the outer strips section will stay roughly the same while the strip length will be reduced from 20 to 5 cm and from 10 to 2.5 cm and even to long macro-pixels of 1.5 mm length. The inner pixel cell size will be reduced by a factor six from 15000 μm^2 to 2500 μm^2 (50×50 or 25×100 μm^2). The six OT barrel layers and five endcap disks are composed of novel p_T-modules with intrinsic capability to distinguish high and low p_T-track segments. The OT has about 42M strips plus 127M macro-pixels, which are complemented by roughly 2B micro-pixels in the IT.

CMS will introduce a Level-1 track trigger that fully reconstructs all $p_T >$ 3 GeV tracks to $\eta < 2.5$ at the 40 MHz bunch crossing rate. Front-end-chips in p_T-modules read channels from two closely spaced sensors in a single frame (strips parallel) and correlate the signals. With the strong bending power of the CMS magnet, only segments of high-p_T tracks (stubs) will be contained in a small 'pass-window' in the second sensor, rf. Figure 9.

With 1.5-mm-long macro-pixels in three layers, primary vertex identification (PV) is possible with a precision of about 1 mm at the L1 trigger. About 80% of the transmitted data are trigger data, for which modern Field Programmable Gate Arrays (FPGAs) fully reconstruct tracks faster than 4 μs.[12,13]

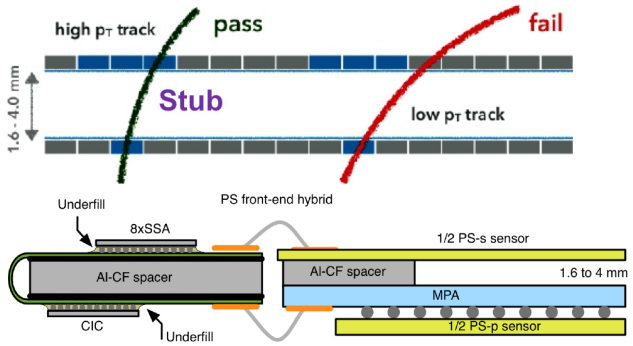

Fig. 9. 'Stubs', depicted in the upper part of the figure, are transmitted to the L1 trigger for every bunch crossing. The lower figure shows a PS-module (Pixel-Strip-sensors: 2.5 cm × 100 μm and 1.5 mm × 100 μm). Signals are routed via flex cables to the other hybrid side, which correlates hits in-situ in the ASICs and identifies p_T 'stubs'.

3.2. *CMS Phase-2 MIP Timing Detector MTD*

With increased pileup, the identification of primary vertices (PV) becomes significantly more difficult, especially in the very forward direction. With pileup of 200, one expects about two primary vertices per millimetre resulting in ∼15% reconstructed PVs to be merged. Collisions within one bunch crossing have a time spread of ∼180 ps, thus precise timing information (time resolution σ_t = 30 – 50 ps) allows to unfold the tracks versus time thereby reducing the pileup to an *effective* value similar to today's pileup. A 4D vertex reconstruction (space + time) are superior to 3D reconstruction especially for low-p_T tracks. CMS estimates a 20% gain in signal yield for di-Higgs events due to improvement in object isolation and b-tagging. The time information also allows particle identification for low-p_T tracks, which is important for dedicated heavy ion runs. The MTD also largely increases the sensitivity to discover long-lived stable particles.

CMS will instrument[14] the barrel region with LYSO crystal bars (3 × 3 × 50 mm^3) read out by 3 × 3 mm^2 SiPMs of 15 μm cell pitch on both crystal ends. The endcap regions will be equipped down to $\eta \simeq 3$ with two layers of Low Gain Amplifier Diodes (LGADs) with cell sizes of 1.3×1.3 mm^2 on sensor sizes of 21×42 mm^2 with 20×20 mm^2 bump bonded readout chips. Both detectors will be operated at a temperature of –30°C or lower realized via CO_2 cooling to limit SiPM dark count rate and LGAD leakage current.

Figure 10 illustrates the global geometry and location of the thin MTD layers. In addition, the time resolution of the barrel electromagnetic calorimeter[15] will be σ_t = 30 ps for energy deposits greater than 30 GeV, while for the endcap high-granularity calorimeter[16] it is expected to be σ_t = 25 ps for deposits equivalent to 50 fC (= 12 MIPs for the 300 μm sensors).

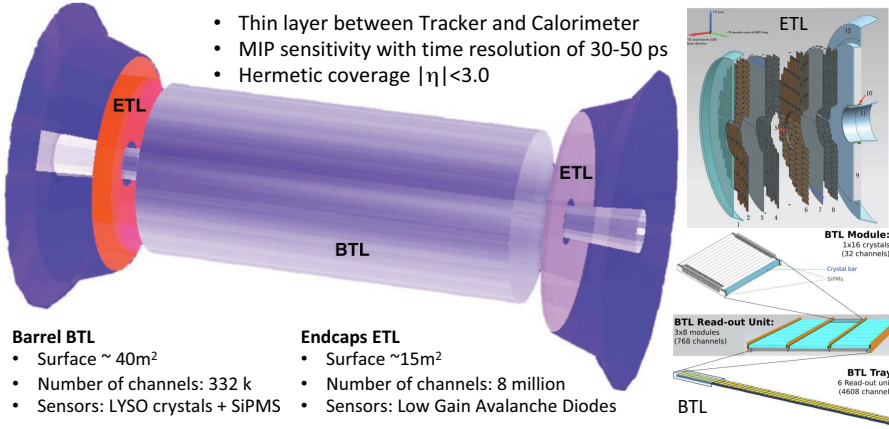

Fig. 10. The HL-LHC MIP Timing Detector MTD. The BTL will be integrated within the Tracker Support Tube, while the ETL will have its own thermal screen between Tracker and HGCAL.[14]

3.3. *CMS Phase-2 Barrel Calorimeter*

Both the homogeneous electromagnetic section (EB), made of lead-tungstate crystals, and the sampling hadronic section (HB), made of brass absorber and scintillator tiles coupled to wavelength-shifting and clear fibers, will withstand the radiation exposure in this barrel region for the entire HL-LHC run with sustainable degradation. The EB Avalanche Photodiodes (APD) and the HB Silicon Photomultipliers (SiPM), installed with new front-end electronics in LS2 as the last item of the CMS Phase-1 upgrade, will also be retained as they will experience a significant but manageable increase in dark current, which will be ameliorated by lowering the operational temperature. The EB front-end electronics and both the EB and HB back-end electronics will be upgraded[15] in LS3 in order to sustain the challenging HL-LHC operating conditions, including the increased L1-trigger rate and latency.

The upgraded EB front end is designed to provide 30 ps timing resolution for photons from di-photon Higgs decays. This will enable precise primary vertex determination, mitigate the effects of the increasing APD dark current noise, suppress anomalous APD signals in the L1 trigger, and provide single crystal information to the L1 trigger (compared to a 5×5 crystal matrix in the legacy system), which will improve electromagnetic shower isolation and permit to retain calorimeter trigger thresholds at the level needed for Higgs precision studies. To carry out this upgrade, the 36 EB *supermodules* shown in Figure 11(a) will be extracted, refurbished, and reinstalled during LS3. Figure 11(b) shows the architecture of the new front-end electronics of EB, which will feature analogue ASICs implemented in 130 nm technology, and digital ASICs and ADCs implemented in 65 nm technology.

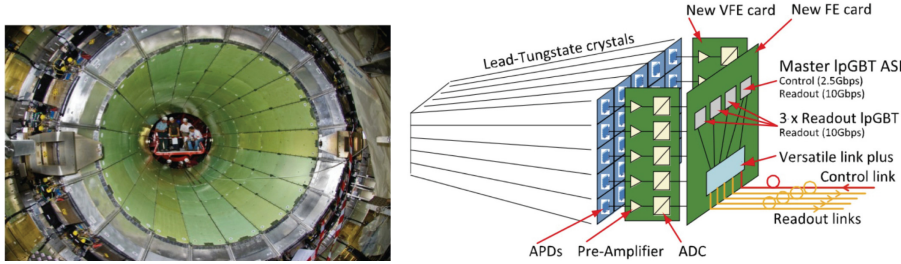

Fig. 11. (a) The 36 wedges (*supermodules*) of the electromagnetic section (EB) of the CMS barrel calorimeter inserted inside the hadronic section (HB). (b) Schematic of the upgrade of the EB front-end electronics architecture for one of the 2448 5×5 crystal matrices.

3.4. *CMS Phase-2 High Granularity Calorimeter*

A long-standing concept for the International Linear Collider, a high granularity calorimeter, based on silicon pad detectors plus scintillator/SiPM cells, will be realised for the CMS Phase-2 Endcap Calorimeter.[16,17] It effectively 'tracks' particles inside the calorimeter, embodying the particle flow concept. The global layout and a photo of a silicon prototype sensor are displayed in Figure 12. Close to 600 m^2 active surface (~25000 silicon modules) will be instrumented with ~6M channels of 0.5 and 1 cm^2 hexagonal pad cells at smaller and larger radius, respectively. The detector is very dense to preserve lateral compactness of showers, and it has a fine lateral granularity to enable two-shower separation and narrow jet identification as well to reduce the

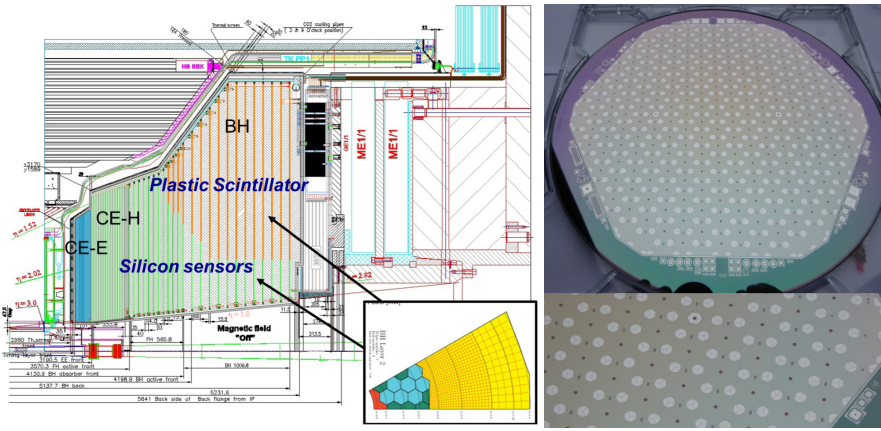

Fig. 12. The CMS Endcap Calorimeter layout is shown on the left; a prototype sensor from an 8 inch silicon wafer is on the right.

inclusion of energy from particles originating in pileup interactions. Fine longitudinal segmentation enables fine sampling of the development of showers, retaining good electromagnetic energy resolution (e.g. for $H \rightarrow \gamma\gamma$), pattern recognition, and discrimination against pileup. For cell signals of 12 fC (about 3 MIPs) a timing precision of 100 ps can be achieved. Streaming reduced data at 40 MHz to the L1 Trigger is achieved by summing up the energy of several cells from every other layer. The electromagnetic part (CE-E) will have 28 sampling layers embedded in Cu/CuW/Pb absorbers, equivalent to around 26 X_0 + 1.7 λ. The hadronic section (CE-H) has 22 layers with stainless steel absorbers, corresponding to about 9 λ. Deeper hadronic layers (BH) at larger radius, with lower radiation exposure, will be equipped with ~400k small plastic scintillator tiles (from 4 to 32 cm^2), each optically coupled to a SiPM. The volume will be kept at a temperature of –30°C via CO_2 cooling. Silicon sensor thicknesses will be 100, 200 and 300 μm, with thinner sensors, being more radiation tolerant, placed at smaller radius. To span the necessary dynamic range of 1 to 5000 MIPs, the readout features a charge amplifier/shaper (low range) plus a time-over-threshold circuit (high range).

3.5. *CMS Phase-2 Muon Detector System*

CMS will significantly overhaul its extensive muon detector and electronics systems to address longevity limitations in the existing systems, increase re-

dundancy, and cope with the increased particle rates due to the higher HL-LHC instantaneous luminosity.[18] The forward region will be extended with high granularity detectors up to $|\eta| = 2.8$ (2.4 today). Figure 13 illustrates the Muon system for the HL-LHC era. Extensive longevity studies show that the DT, CSC and RPC chambers will remain operational during the full HL-LHC period with reduced voltages, while their front-end electronics might not withstand the total expected radiation. New electronics will increase rate capability and trigger latency as required, improve time resolution for RPCs (1.5 ns), and make the DT time resolution (2 ns) available at L1 trigger. Trigger primitives of DTs and RPC will be generated in off-detector FPGA systems to enable more complex topologies, e.g. improving the sensitivity for discovering long-lived stable particles. The high spatial resolution and MHz/cm^2 capability of the GEM technology is crucial for instrumenting the high-η region. Three GEM stations (GE1/1, G2/1 and ME0) plus two improved RPC stations (RE3/1 and RE4/1) at high η will significantly improve trigger efficiency and, due to better spatial resolution, p_T resolution. The CSC upgrade, installation of GE1/1 and of GEM and RPC endcap services is taking place during LS2.

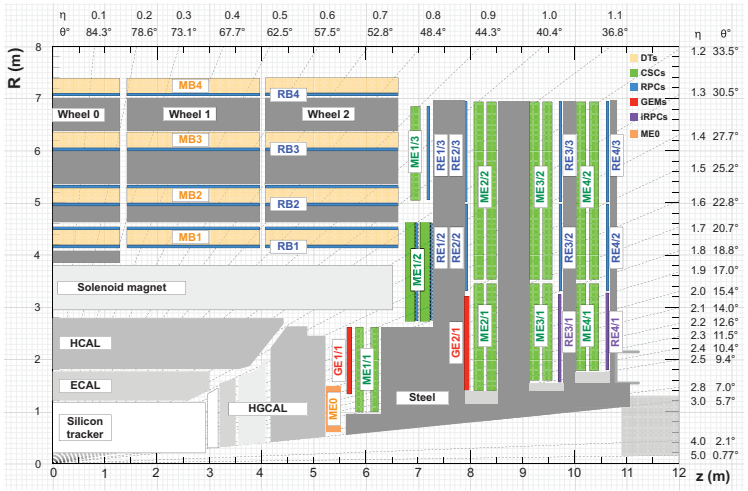

Fig. 13. The HL-LHC Muon Detector System. An R-z cross section of a quadrant of the CMS detector, including the new Phase-2 upgrades (RE3/1, RE4/1, GE1/1, GE2/1, ME0). The locations of the various muon stations are shown in color (MB = DT = Drift Tubes, ME = CSC = Cathode Strip Chambers, RB and RE = RPC = Resistive Plate Chambers, GE and ME0 = GEM = Gas Electron Multiplier).

3.6. *CMS Phase-2 Trigger and Data Acquisition*

A new Trigger and Data Acquisition (TDAQ) system[19,20] will process data at an unprecedented rate of 50 Tb/s, corresponding to the Level-1 trigger event rate of 750 kHz, to select and record events at 7.5 kHz. The Phase-2 TDAQ system will continue to be based on a two-level trigger strategy. The custom hardware Level-1 (L1) trigger will take full advantage of advances in FPGA and optical link technologies. The inputs to the L1 trigger, namely the Trigger Primitives (TPs), are generated at 40 MHz in the subdetector back-end electronics, based on the Advanced Telecommunications Computing Architecture (ATCA) standard. For the first time, tracking information from the Outer Tracker will be sent to the L1 trigger and will be crucial for keeping trigger thresholds and efficiencies consistent with LHC Run 1 values. High-resolution clusters will be produced from the Endcap and Barrel Calorimeter TPs. Muon TPs will incorporate data from the additional chambers covering pseudorapidity up to $|\eta| = 2.8$. A new Correlator Trigger system will match tracks with the calorimeter and muon information, apply object identification algorithms, and provide a list of sorted trigger objects to a Global Trigger. This will apply sophisticated algorithms, particle flow and machine learning to produce an L1-accept signal with a fixed latency of 12.5 μs to be distributed to the subdetector backend electronics, initiating readout through a standardized ATCA data concentrator board included in every subdetector back-end crate. Then, the High-Level Trigger (HLT)[20] will process full detector event data through software algorithms running asynchronously on standard processors. Accepted events will be recorded for efficient long-term storage and subsequent offline reconstruction.

3.7. *CMS Precision Proton Spectrometer PPS for HL-LHC*

After successful operation of the Precision Proton Spectrometer (PPS) since 2016, the CMS Collaboration is planning to pursue the study of central exclusive production (CEP) events, $pp \rightarrow pXp$, at the HL-LHC with detection of the state X in the central detectors and of the leading protons in the PPS stations with a large, not continuous, acceptance on masses of X from ~50 GeV to ~3 TeV.[21] More specifically, we target a kinematic acceptance for the centrally produced X state of 44–160 GeV with a cryogenic ("cold") station at 420 m, and 264–370 GeV, 520–960 GeV, and 1–2.72 TeV with three non-cryogenic

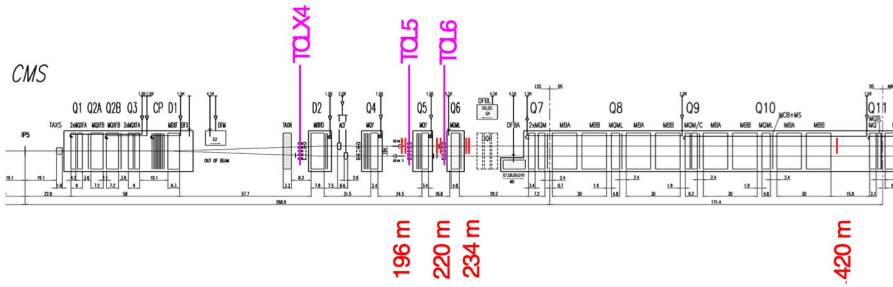

Fig. 14. Phase-2 layout of Long Straight Section LSS5, where the PPS detectors are planned to be located.

("warm") stations at 234, 220 and 196 m, respectively. The foreseen locations of the detectors, which will be on both sides of IP5, are indicated in Figure 14. Tracking and timing detectors are planned. The Higgs mass is only accessible with the 420 m station in the cold section.

The three warm stations can be instrumented with upgraded Roman Pot technology while the cold station needs a cryogenic bypass as the signal protons arrive in between the beam pipes, and new development is necessary. The required sensitive area is only a few cm^2 but with PU = 200, pad sizes should be in the order of 100–200 μm and sensor radiation tolerant up to 1.5×10^{16} n_{eq} /cm^2. The preferred technologies are diamond for timing and 3D for tracking. To achieve a good vertex determination via time of flight, the goal is to reach a σ_T of 15–20 ps/arm with ~15 planes (50–60 ps/plane). The MTD in the central detector is instrumental to make the track association.

4. The HL-LHC Upgrades of the LHCb Detector

The LHCb Upgrade II programme[22] aims to make full use of the capabilities of a forward acceptance detector during the HL-LHC operational period, foremost in its core areas of *CP* violation and rare decays in flavour physics. Its capabilities range far beyond these into forward and high-p_T physics, spectroscopy, heavy ion and fixed taget physics, dark-sector searches and beyond. The LHCb Upgrade I is currently under construction and will start data taking in 2022 after LHC Long Shutdown 2 (LS2). The future LHCb for the HL-LHC era will be installed in a consolidation phase during LS3, with primary operations of LHCb Upgrade II starting in Run 5 after LS4 operating

at an instantaneous luminosity of $1.5 \times 10^{34}\,\mathrm{cm}^{-2}\,\mathrm{sec}^{-1}$, nearly an order of magnitude above Upgrade I. LHCb Upgrade II will accumulate a data sample corresponding to a minimum of $300\,\mathrm{fb}^{-1}$. The general concepts were presented in an Expression of Interest in 2017,[22] and a Physics Case in 2018.[23] The data sample collected by the end of the HL-LHC period will be more than a factor thirteen higher than that collected in the pre-HL-LHC period. The energy scale probed through precision measurements scales as the fourth root of the sample size, so the step from the pre-HL-LHC to the post-HL-LHC, and post Belle II, period corresponds to a factor of 1.9 or more in reach or corresponding to an LHC energy increase from 14 TeV to 27 TeV.

4.1. *Tracking with timing detectors*

At a luminosity of $2 \times 10^{34}\,\mathrm{cm}^{-2}\mathrm{s}^{-1}$, the maximum considered, the mean number of visible proton-proton interactions per crossing will be 56, producing around 2500 charged particles within the LHCb acceptance. Efficient real-time reconstruction of charged particles and interaction vertices represents a significant challenge. It is foreseen to modify the existing spectrometer components to increase the granularity, reduce the amount of material and to exploit the use of precision timing.[22]

4.1.1. *The vertex detector*

The LHCb upgrade physics programme is reliant on an efficient and precise vertex detector (VELO) that enables real time reconstruction of tracks in the software trigger system. To cope with the large increase in pile-up, new techniques to assign correctly each b hadron to the primary vertex (PV) will be realized by the development of a new 4D hybrid pixel detector with enhanced rate and timing capabilities in the ASIC and sensor. Improvements in the mechanical design of the Upgrade II VELO will allow for periodic module replacement. The principle behind the use of timing information for PV association is illustrated, for a single event, in Figure 15a. Studies show that without timing, the Upgrade II PV mis-association levels may reach $\sim 20\%$, and this can be reduced to $\sim 5\%$ with a timing precision of 50–100 ps. Studies have also shown that the track reconstruction efficiency and fake rate can be addressed by decreasing the pixel pitch from the current 55 μm, particularly for the innermost region of the VELO. Timing will sped up track reconstruction,

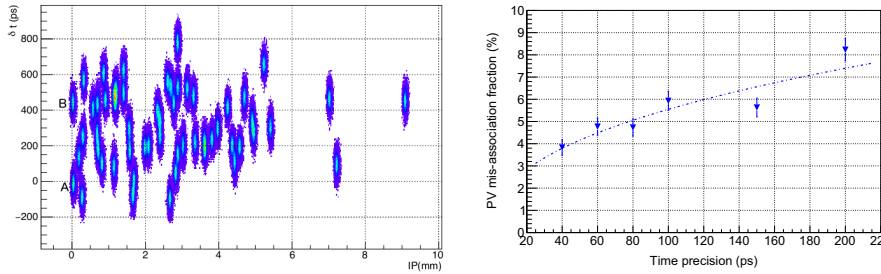

(a) (b)

Fig. 15. (a) Example event containing a $B^0 \to \pi^+\pi^-$ candidate, illustrating the PV association challenge. Each PV is drawn as a 2D Gaussian distribution with the appropriate values and uncertainties for both spatial (x-axis) and temporal (y-axis) metrics used to associate the B meson to a single origin PV. Adding the temporal information allows the correct PV ['A', closest to $(0, 0)$] to be identified where the spatial information alone would lead to the wrong choice ('B').
(b) Fraction of $B^0 \to \pi^+\pi^-$ candidates which are associated with an incorrect primary vertex in Upgrade II conditions ($\mathcal{L} = 1.5 \times 10^{34}\,\mathrm{cm}^{-2}\mathrm{s}^{-1}$), for the outer radial region ($20 < r < 35\,\mathrm{mm}$) of the VELO, to be compared with the 20% PV mis-association fraction corresponding to a detector with no time information.

reducing drastically combinatorics at an early stage, saving CPU resources. Also a 'mixed' solution is considered where the inner region has a smaller pitch (emphasising resolution) and the outer region has a larger pitch emphasising more precise timing. Studies of the performance are shown in Figure 15b.

4.1.2. *Downstream tracking*

Changes to the downstream tracking system are also foreseen. In Upgrade I this comprises a silicon strip detector located upstream (UT) and three tracking stations located downstream of the magnet (T-stations) realised by a twelve-layer scintillating fibre tracker (SciFi). This covers the full acceptance, corresponding to $30\,\mathrm{m}^2$ per layer. In conjunction with the VELO, these stations provide a high precision momentum measurement and provide the track directions as input to the particle identification systems. For Upgrade II the higher occupancies necessitate increased detector granularity. Second, the rate of incorrect matching of upstream and downstream track segments needs to be minimised. The inner part of the T-stations will be replaced with a high granularity

silicon detector, with the large area covered by scintillating fibres. Based upon occupancy studies it is proposed to cover the inner region with six planes of silicon.[22] The design of this new silicon detector is expected to be based on HV-CMOS technology, the first of its kind at the LHC. Pixels Sizes of around $300 \times 100\,\mu$m are under study.

4.1.3. *Magnet stations*

For Upgrade Ib in LS3, it is proposed to extend the spectrometer coverage for low momentum tracks (for example the slow pion from the decay $D^{*+} \rightarrow D^0\pi^+$) by instrumenting the internal surfaces of the magnet with scintillating fibres. A spatial resolution of the order of a mm is sufficient in the bending-plane to obtain the required momentum resolution. The use of a stereo arrangement of layers will be implemented to achieve the required y segmentation.

4.2. *Particle identification*

High quality particle identification (PID) is essential for almost all precision flavour measurements. These developments will improve granularity and, for certain subdetectors, add fast timing of the order of a few tens of picoseconds, in order to associate signals with one, or a small number, of pp interactions in the bunch crossing.

4.2.1. *Hadron identification: the RICH system and the TORCH*

The RICH system of Upgrade II will be a natural evolution of the current detectors and those being constructed for Upgrade I. There will be two counters, an upstream RICH 1 optimised for lower momentum tracks, and a downstream RICH 2, both occupying essentially the same footprint as now. Higher granularity and fast timing photodetectors will resolve the increased track multiplicity. Several candidate technologies are under consideration, with SiPMs being a leading contender. Other possibilities include vacuum devices such as MCPs, HPDs and MaPMTs.

As well as reducing the occupancy it will be necessary to improve the Cherenkov angle resolution by around a factor of three in both counters with

respect to the specifications of Upgrade I. This goal can be achieved by redesigning the optics ensuring that the response of the photodetectors is weighted towards longer wavelengths, and taking advantage of the smaller pixel size.

There is an exciting possibility, under consideration, to enhance the low-momentum hadron-identification capabilities of the experiment by installing a TORCH detector, measuring time-of-flight through detecting internally reflected Cherenkov light produced in a thin (∼1 cm) quartz plane with MCP photodetectors. A time resolution of 70 ps per photon and an expected yield of ∼30 photons per track will allow for kaons and low-momentum proton identification in the region below 10 GeV/c. These improvements would benefit flavour tagging, reconstruction of multi-body final states, physics with baryons and spectroscopy studies. A suitable location for the TORCH within LHCb would be upstream of RICH 2.

4.2.2. *Electromagnetic calorimeter*

The electron, photon and π^0 identification provided by the current electromagnetic calorimeter (ECAL) has proved of great importance. The principal challenges for the ECAL at Upgrade II will be threefold. Firstly, the radiation environment will be extremely severe, with a total dose of around 200 Mrad foreseen for the innermost modules. Indeed, severe degradation in performance is already expected for these innermost modules by the time of LS3, requiring replacement. Secondly, the very high luminosity of $10^{34}\,\mathrm{cm}^{-2}\mathrm{s}^{-1}$ operation will lead to overlapping showers and a corresponding degradation in energy resolution and shower finding efficiency. This problem can be tackled by reducing the Molière radius of the converter and moving to a smaller cell size, for example $2{\times}2\,\mathrm{cm}^2$ in the inner region. Finally, the high number of candidates in every event, for example of π^0 mesons, will lead to an unacceptably large combinatoric background. Hence fast timing information will be essential to associate the candidates to individual pp interactions in the bunch crossing.

One option being pursued is a homogeneous crystal calorimeter with longitudinal segmentation. Materials are being investigated, which offer good radiation hardness, excellent energy resolution and very fast response. Another possibility is a sampling calorimeter, either Shashlik or SpaCal, with a

tungsten-alloy converter, with a crystal component for providing a fast-timing signal. An alternative source of fast timing would be a preshower layer involving silicon pads.

4.2.3. *The muon system*

Operating the current muon system in Upgrade I conditions would lead to a degraded performance due to dead-time induced inefficiencies and an increased rate of ghost hits, all coming from the higher background flux. Future improvements comprise of a modification to the electronics to increase the granularity, the replacement of certain detectors with new pad chambers, and additional shielding around the beam pipe. For Upgrade II luminosities, extra shielding will be required to suppress the flux of punchthrough. This can be achieved by replacing the HCAL with up to 1.7 m of iron, which would provide an additional four interaction lengths compared to the current situation. New detectors will be installed in the innermost region of all stations, with a design possessing both high granularity and high rate capabilities. A promising solution is the micro-resistive WELL detector (μ-RWELL[24]), a novel MPGD with good prospects for satisfying these criteria. In the lower flux region μ-RWELL or new MWPC detectors could be installed.

4.3. *Trigger and data processing*

At an instantaneous luminosity of up to $2 \times 10^{34}\text{cm}^{-2}\text{s}^{-1}$, the LHCb detector is expected to produce up to $400 - 500$ Tb of data per second, which will have to be processed in real time and reduced by at least $4 - 5$ orders of magnitude before recording the remainder to permanent storage. The ongoing evolution of radiation-hard optical links and commercial networking technology, is expected to allow transferring this volume of the data off the detector and into a processor farm. The Upgrade II data processing will be based around pile-up suppression, in which detector hits not associated with the individual pp interaction of interest are discarded as early as possible in the processing chain.

Timing information from the detectors allows for a particularly fast separation of reconstructed objects according to the pp interaction that produced them LHCb has already demonstrated the ability to perform a full offline-

quality detector alignment, calibration, and reconstruction in near-real-time in Run 2, as well as the ability to perform precision physics measurements using this real-time data processing. Given the ongoing trend towards more and more heterogeneous computing architectures, with CPU server farms increasingly supplemented with GPU or FPGA accelerators, it will be critical to study such hybrid architectures.

5. The HL-LHC Upgrade of the ALICE Detector

During LS2, the ALICE Collaboration is enhancing its physics capabilities with a major upgrade of the detectors, electronics and data-processing systems which will improve the precision of the extracted characteristics of the high density, high temperature phase of strongly interacting matter, the quark-gluon plasma (QGP), together with the exploration of new phenomena in Quantum Chromodynamics (QCD). The major focus for Runs 3 and 4 will be on rare probes such as heavy-flavour particles, quarkonium states, real and virtual photons and low-mass dileptons as well as on the study of jet quenching and exotic nuclear states.[25,26] The ALICE upgrade strategy is formulated under the assumption that, in Run 3, the LHC will progressively increase the luminosity of Pb beams to reach an interaction rate of 50 kHz (instantaneous luminosity of 6×10^{27} cm^{-2}s^{-1}). ALICE will then be able to accumulate ten times more integrated luminosity (more than 13 nb^{-1}) than what has been collected so far.

5.1. *General layout of upgraded ALICE*

Figure 16 shows a sketch of the upgraded ALICE experimental setup which includes a newly built Inner Tracking System (ITS) with a new high-resolution, low-material-budget silicon tracker, which extends to forward rapidities with the new Muon Forward Tracker (MFT), an upgraded Time Projection Chamber (TPC) with Gas Electron Multiplier (GEM) detectors along with a new readout chip for faster readout, new Fast Interaction Trigger (FIT) detector, new readout electronics for the muon spectrometer, Time-of-flight (TOF) detector, Transition Radiation Detector (TRD), Electromagnetic Calorimeter (EMCAL), Photon Spectrometer (PHOS), Zero Degree Calorimeter (ZDC), and an integrated online-offline (O^2) computing system to process and store the large data volume. The beryllium beam pipe near the interaction point (IP)

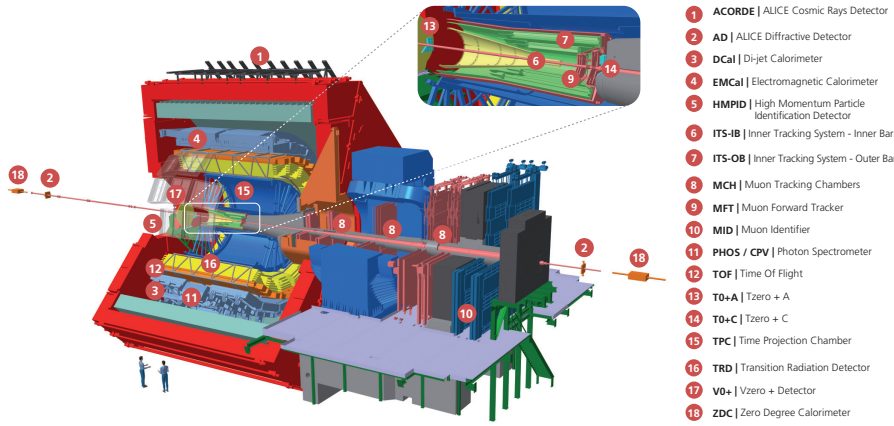

Fig. 16. ALICE upgraded experimental set-up for the HL-LHC.

is also newly installed with a smaller outer radius of 19 mm compared to the former one of 29.8 mm.

5.2. *Inner tracking with the ITS and the MFT*

The new ITS and the MFT are two all-pixel detectors (see Figure 17) based on CMOS monolithic active pixel sensor (MAPS) technology. In the MAPS technology, both the sensor for charge collection and the readout circuit for digitization are hosted in the same piece of silicon instead of being bump-bonded together. The chip developed by ALICE, and called ALPIDE, uses a 180 nm CMOS process. With this chip, the silicon material budget per layer is reduced by a factor of seven compared to the present ITS. The ALPIDE chip is 15×30 mm^2 in size and contains more than half a million pixels organized in 1024 columns and 512 rows. Its low power consumption (<40 mW/cm^2) and excellent spatial resolution (5 μm) optimally matches the requirements for measuring rare probes such as heavy flavour hadrons in an environment with a large track density.

The ITS (covering the region, $\eta < 1.5$) consists of seven cylindrical layers of ALPIDE chips with 12.5 billion pixels, covering a total area of 10 m^2. The pixel chips are installed on staves with radial distances ranging from 22 mm to 400 mm to the IP. The new beam pipe allows for the first detection layer to be placed closer to the IP at a radius of 22.4 mm compared to 39 mm during Runs

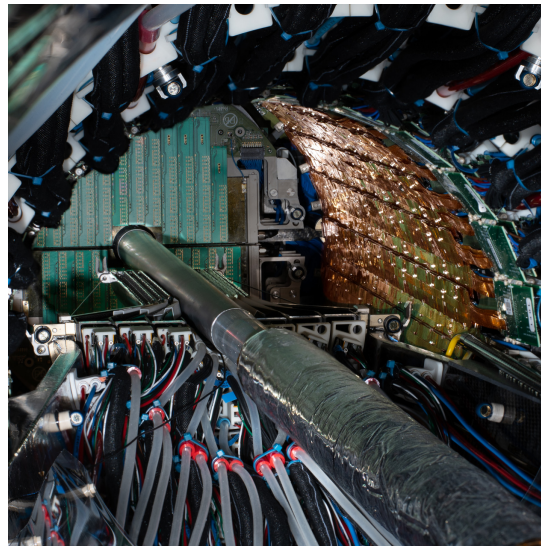

Fig. 17. The figure shows the installed inner (left, middle) and outer (gold colour) barrels of the ITS, along with the MFT (green panel) in the ALICE cavern.

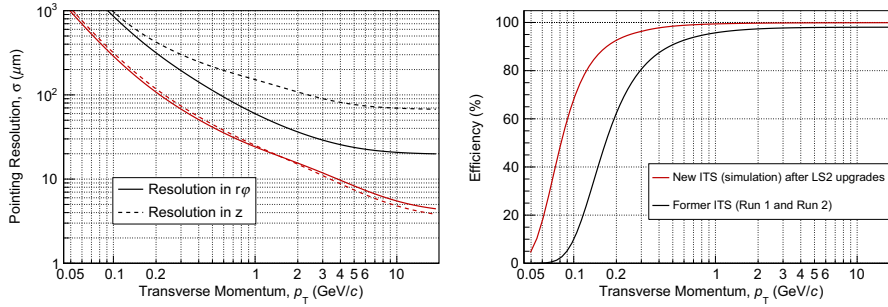

(a) (b)

Fig. 18. Expected pointing resolution (a) and efficiency (b) of the upgraded ALICE ITS as a function of the track p_T.

1 and 2. The new ITS detector will improve the impact parameter resolution (Figure 18a) by a factor of three in the transverse plane and by a factor of five along the beam axis. It will also extend the tracking capabilities to much lower p_T, allowing ALICE to perform measurements of heavy-flavour hadrons down to zero p_T (see Figure 18b).

The new MFT detector, located at forward rapidity ($2.45 < \eta < 3.6$), is designed to add vertexing capabilities to the muon spectrometer and will enable several new measurements. As an example, it will allow to distinguish J/ψ mesons that are produced directly in the collision from those that come from decays of mesons which contain a beauty quark. The MFT consists of five disks, each with two MAPS detection planes, placed perpendicular to the beam axis between the IP and the hadron absorber of the muon spectrometer.

5.3. *Novel configuration with GEM detectors for the TPC and improved readout*

The TPC is the key device for tracking and charged particle identification in ALICE. It consists of a 90 m^3 cylinder filled with gas and divided in two drift regions by the central electrode located at its axial centre. The field cage secures the uniform electric field along the z-axis. The new TPC readout chambers employ a novel configuration of stacks of four GEM detectors (see Figure 19) instead of multi-wire proportional chambers (MWPC). That will allow for continuous readout at 50 kHz with Pb–Pb collisions at no cost to detector performance. The replacement of the chambers in the TPC from MWPC to the GEM detectors had been one of the major activities of the LS2 period. At the end of the year 2020, a major milestone was achieved with the completion of the TPC upgrade, after many years of intense R&D, construction and assembly.

The readout of the TPC as well as the one of the muon chambers is performed by SAMPA, a newly developed, 32-channel front-end analog-to-

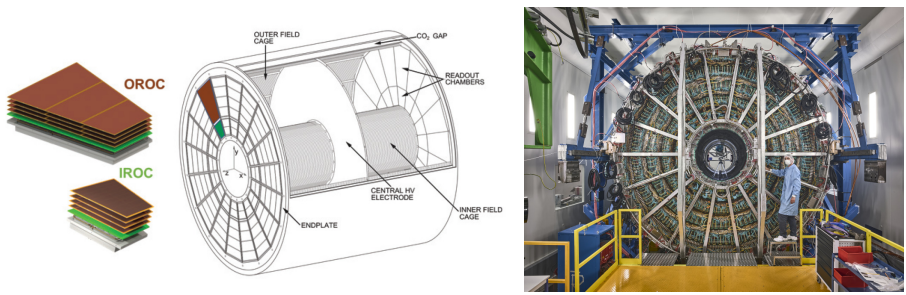

Fig. 19. Configuration of the GEM detectors employed for the ALICE TPC (left) and a photograph showing the installed readout chambers (right).

digital converter (ADC) ASIC with integrated digital signal processor. The newly designed ALICE readout system presents a change in general approach as all Pb–Pb collisions that are produced in the accelerator, at a rate of 50 kHz rate will be read out in a continuous stream. Triggered readout will be used by only a fraction of the detectors and for commissioning and calibration runs and for proton-proton collisions. The central trigger processor (CTP) is being upgraded to accommodate the higher interaction rate.

5.4. *Fast interaction trigger (FIT)*

The Fast Interaction Trigger (FIT) serves as an interaction trigger, online luminometer, initial indicator of the vertex position, and the forward multiplicity counter. In the offline mode, it provides the precise collision time for the TOF-based particle identification, yields the centrality and interaction plane, and measures cross sections of diffractive processes. The FIT relies on three state-of-the-art detector technologies underpinning components grouped into five arrays surrounding the LHC beamline, at -1, +3, +17, and -19 metres from the interaction point as shown in the left panel of Figure 20. Among the three components that make up the FIT detector, the FT0 is the fastest: comprising 208 optically separated quartz radiators, its expected time resolution for high-multiplicity heavy-ion collisions is about 7 picoseconds. The second component, is a segmented scintillator called FV0. Finally, the Forward Diffractive Detector (FDD), consisting of two nearly identical scintillator arrays, can tag photon-induced or diffractive processes by recognising the absence of activity in the forward direction. A photograph of the installed FV0 and FT0-A is shown in the right panel of Figure 20.

5.5. *An integrated online-offline computing system (O^2)*

The improved ALICE detector is capable of collecting events at 100 times faster rate during LHC Run-3 compared to previous Runs (1 and 2). The total data volume produced by the front-end cards of the detectors will increase significantly, reaching a sustained data throughput of up to 3 TB/s. This necessitated the development and implementation of a completely new readout and computing system. The ALICE computing model is redesigned in order to minimise the data volume from the detectors as early as possible during the

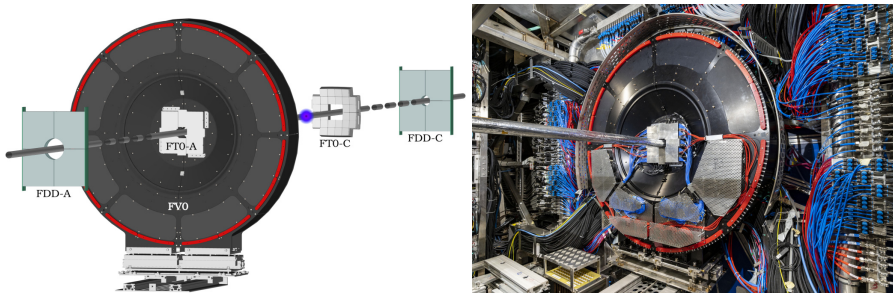

Fig. 20. Layout of the new Fast Interaction Trigger (FIT) of ALICE and a photograph showing the installed detector in the cavern.

data processing. This is achieved by online processing of the data including detector calibration and reconstruction of events in several steps synchronously with data taking. At its peak, the estimated data throughput to the mass storage is 90 GB/s. To reach this goal, a new computing facility is being installed on the surface, near the experiment. It will feature a data storage system with a capacity large enough to accommodate an important fraction of a full year data taking. It will also provide the interface to the permanent data storage at the Tier-0 computing centre at CERN as well as other data processing centres.

5.6. *ALICE upgrade during Long Shutdown 3*

During LS3 period, ALICE will further upgrade[27] ITS to a newly designed vertex detector consisting of curved wafer-scale ultra-thin silicon sensors arranged in perfectly cylindrical layers, featuring an unprecedented low material budget of 0.05% radiation length per layer, with the innermost layer positioned at only 18 mm radial distance from the interaction point. Such a novel detector (ITS3), replacing the three innermost layers of the ITS would significantly improve the measurement of low momentum charmed hadrons and low-mass dielectrons in heavy-ion collisions.

In addition, a new forward electromagnetic and hadronic calorimeter (FoCal)[28] covering $3.2 < \eta < 5.8$ will be installed during LS3, which will provide ALICE with unique capabilities to measure small-x gluon distributions via prompt photon production and will significantly enhance the scope of ALICE for inclusive and correlation measurements with mesons, photons, and jets to explore the dynamics of hadronic matter at small x down to $\sim 10^{-6}$.

5.7. *ALICE during the HL-LHC era*

The running scenario in HL-LHC era foresees a high statistics Pb-Pb collision sample of at least 13 nb^{-1} accompanied with O-O as well as pp, p-O, and p-Pb collisions.[26] The future plan after Run 4 calls for a compact, next-generation multipurpose detector as a follow-up to the ALICE experiment.[29] The aim is to build a nearly massless barrel detector consisting of truly cylindrical layers based on curved wafer-scale ultra-thin silicon sensors with MAPS technology. This detector is conceived to handle luminosities a factor of 20 to 50 times higher than what will be possible for the upgraded ALICE detector, enabling a new, rich physics program.

The major upgrades during the LS2 and LS3 will allow ALICE to enter the HL-LHC era with a more precise, reliable and faster experimental set-up. The experiment will provide high-precision measurements and pave the way for the next generation of nearly mass-less barrel detectors.

References

1. G. Apollinari, I. Béjar Alonso, O. Brüning, M. Lamont, and L. Rossi, *High-Luminosity Large Hadron Collider (HL-LHC): Preliminary Design Report*. CERN Yellow Reports: Monographs, CERN, Geneva (2015). doi: 10.5170/CERN-2015-005. URL `http://cds.cern.ch/record/2116337`.
2. O. Brüning and L. Rossi, eds., *The High Luminosity Large Hadron Collider: the new machine for illuminating the mysteries of Universe*. vol. 24 (2015). ISBN 978-981-4675-46-8, 978-981-4678-14-8. doi: 10.1142/9581.
3. I. Béjar Alonso, O. Brüning, P. Fessia, M. Lamont, L. Rossi, L. Tavian, and M. Zerlauth, eds., *High-Luminosity Large Hadron Collider (HL-LHC): Technical Design Report*. vol. 10/2020 (2020). doi: 10.23731/CYRM-2020-0010.
4. The ATLAS Collaboration. Technical Design Report for the ATLAS Inner Tracker Pixel Detector. Technical Report CERN-LHCC-2017-021. ATLAS-TDR-030, CERN, Geneva (June, 2018). URL `https://cds.cern.ch/record/2285585`.
5. The ATLAS Collaboration. Technical Design Report for the ATLAS Inner Tracker Strip Detector. Technical Report CERN-LHCC-2017-005. ATLAS-TDR-025, CERN, Geneva (April, 2017). URL `https://cds.cern.ch/record/2257755`.
6. The ATLAS Collaboration. ATLAS Liquid Argon Calorimeter Phase-II Upgrade Technical Design Report. Technical Report CERN-LHCC-2017-018. ATLAS-TDR-027, CERN, Geneva (June, 2018). URL `https://cds.cern.ch/record/2285582`.

7. The ATLAS Collaboration. Technical Design Report for the Phase-II Upgrade of the ATLAS Tile Calorimeter. Technical Report CERN-LHCC-2017-019. ATLAS-TDR-028, CERN, Geneva (June, 2018). URL https://cds.cern.ch/record/2285583.
8. The ATLAS Collaboration. Technical Design Report for the Phase-II Upgrade of the ATLAS Muon Spectrometer. Technical Report CERN-LHCC-2017-017. ATLAS-TDR-026, CERN, Geneva (December, 2017). URL https://cds.cern.ch/record/2285580.
9. The ATLAS Collaboration. Technical Design Report: A High-Granularity Timing Detector for the ATLAS Phase-II Upgrade. Technical Report CERN-LHCC-2020-007. ATLAS-TDR-031, CERN, Geneva (June, 2020). URL https://cds.cern.ch/record/2719855.
10. The ATLAS Collaboration. Technical Design Report for the Phase-II Upgrade of the ATLAS Trigger and Data Acquisition System. Technical Report CERN-LHCC-2017-020. ATLAS-TDR-029, CERN, Geneva (June, 2018). URL https://cds.cern.ch/record/2285584.
11. The CMS Collaboration, Particle-flow reconstruction and global event description with the CMS detector, *JINST*. **12**(10), P10003 (2017). doi: 10.1088/1748-0221/12/10/P10003.
12. The CMS Collaboration. The Phase-2 Upgrade of the CMS Tracker. Technical Report CERN-LHCC-2017-009. CMS-TDR-014, CERN, Geneva (Jun, 2017). URL https://cds.cern.ch/record/2272264.
13. I. Tomalin et al., An FPGA based track finder for the L1 trigger of the CMS experiment at the High Luminosity LHC, *JINST*. **12**, P12019 (2017). doi: 10.1088/1748-0221/12/12/P12019.
14. The CMS Collaboration. A MIP Timing Detector for the CMS Phase-2 Upgrade. Technical Report CERN-LHCC-2019-003. CMS-TDR-020, CERN, Geneva (Mar, 2019). URL http://cds.cern.ch/record/2667167.
15. The CMS Collaboration. The Phase-2 Upgrade of the CMS Barrel Calorimeters. Technical Report CERN-LHCC-2017-011. CMS-TDR-015, CERN, Geneva (Sep, 2017). URL https://cds.cern.ch/record/2283187.
16. The CMS Collaboration. The Phase-2 Upgrade of the CMS Endcap Calorimeter. Technical Report CERN-LHCC-2017-023. CMS-TDR-019, CERN, Geneva (Nov, 2017). URL https://cds.cern.ch/record/2293646.
17. The CMS Collaboration. Technical Proposal for the Phase-II Upgrade of the CMS Detector. Technical Report CERN-LHCC-2015-010. LHCC-P-008. CMS-TDR-15-02, Geneva (Jun, 2015). URL https://cds.cern.ch/record/2020886.
18. The CMS Collaboration. The Phase-2 Upgrade of the CMS Muon Detectors. Technical Report CERN-LHCC-2017-012. CMS-TDR-016, CERN, Geneva (Sep, 2017). URL https://cds.cern.ch/record/2283189.
19. The CMS Collaboration. The Phase-2 Upgrade of the CMS Level-1 Trigger. Technical Report CERN-LHCC-2020-004. CMS-TDR-021, CERN, Geneva (June, 2020). URL http://cds.cern.ch/record/2714892.
20. CMS Collaboration. The Phase-2 Upgrade of the CMS Data Acquisition and High Level Trigger. Technical report, CERN, Geneva (Mar, 2021). URL https://cds.cern.ch/record/2759072.

21. The CMS Precision Proton Spectrometer at the HL-LHC – Expression of Interest. Technical report (Mar, 2021). URL https://cds.cern.ch/record/2750358.
22. R. Aaij et al., Expression of Interest for a Phase-II LHCb Upgrade: Opportunities in flavour physics, and beyond, in the HL-LHC era. (CERN-LHCC-2017-003) (2017).
23. R. Aaij et al., Physics case for an LHCb Upgrade II - Opportunities in flavour physics, and beyond, in the HL-LHC era (2018).
24. G. Bencivenni, R. De Oliveira, G. Morello, and M. Poli Lener, The micro-Resistive WELL detector: a compact spark-protected single amplification-stage MPGD, *JINST*. **10**, P02008 (2015). doi: 10.1088/1748-0221/10/02/P02008.
25. B. Abelev et al., Upgrade of the ALICE Experiment: Letter Of Intent, *J. Phys. G*. **41**, 087001 (2014). doi: 10.1088/0954-3899/41/8/087001.
26. Z. Citron et al., *Report from Working Group 5: Future physics opportunities for high-density QCD at the LHC with heavy-ion and proton beams*, In eds. A. Dainese, M. Mangano, A. B. Meyer, A. Nisati, G. Salam, and M. A. Vesterinen, *Report on the Physics at the HL-LHC, and Perspectives for the HE-LHC*, vol. 7, pp. 1159–1410 (Dec, 2019). doi: 10.23731/CYRM-2019-007.1159.
27. The ALICE Collaboration. Letter of Intent for an ALICE ITS Upgrade in LS3. Technical Report CERN-LHCC-2019-018; LHCC-I-034, CERN, Geneva (December, 2019). URL https://cds.cern.ch/record/2703140.
28. The ALICE Collaboration. Letter of Intent: A Forward Calorimeter (FoCal) in the ALICE experiment. Technical Report CERN-LHCC-2020-009; LHCC-I-036, CERN, Geneva (June, 2020). URL https://cds.cern.ch/record/2719928.
29. D. Adamova et al., A next-generation LHC heavy-ion experiment (Jan, 2019).